precipitation projections was explained by the differences in global model boundary conditions, although much of the spread in projected summer precipitation was explained by RCM. This underlines the importance of both the quality of the boundary conditions and the downscaling method.

9.7 Climate Sensitivity and Climate Feedbacks

An overall assessment of climate sensitivity and transient climate response is given in Box 12.2. Observational constraints based on observed warming over the last century are discussed in Section 10.8.2 and shown in Box 12.2, Figure 2.

9.7.1 Equilibrium Climate Sensitivity, Idealized Radiative Forcing, and Transient Climate Response in the Coupled Model Intercomparison Project Phase 5 Ensemble

Equilibrium climate sensitivity (ECS) is the equilibrium change in global and annual mean surface air temperature after doubling the atmospheric concentration of CO_2 relative to pre-industrial levels. In the AR4, the range in equilibrium climate sensitivity of the CMIP3 models was 2.1°C to 4.4°C, and the single largest contributor to this spread was differences among modelled cloud feedbacks. These assessments carry over to the CMIP5 ensemble without any substantial change (Table 9.5).

The method of diagnosing climate sensitivity in CMIP5 differs fundamentally from the method employed in CMIP3 and assessed in the AR4 (Randall et al., 2007). In CMIP3, an AGCM was coupled to a non-dynamic mixed-layer (slab) ocean model with prescribed ocean heat transport convergence. CO_2 concentration was then instantaneously doubled, and the model was integrated to a new equilibrium with unchanged implied ocean heat transport. While computationally efficient, this method had the disadvantage of employing a different model from that used for the historical simulations and climate projections. However, in the few comparisons that were made, the resulting disagreement in ECS was less than about 10% (Boer and Yu, 2003; Williams et al., 2008; Danabasoglu and Gent, 2009; Li et al., 2013a). In CMIP5, climate sensitivity is diagnosed directly from the AOGCMs following the approach of Gregory et al. (2004). In this case the CO_2 concentration is instantaneously quadrupled and kept constant for 150 years of simulation, and both equilibrium climate sensitivity and RF are diagnosed from a linear fit of perturbations in global mean surface temperature to the instantaneous radiative imbalance at the TOA.

The transient climate response (TCR) is the change in global and annual mean surface temperature from an experiment in which the CO_2 concentration is increased by 1% yr^{-1}, and calculated using the difference between the start of the experiment and a 20-year period centred on the time of CO_2 doubling. TCR is smaller than ECS because ocean heat uptake delays surface warming. TCR is linearly correlated with ECS in the CMIP5 ensemble (Figure 9.42), although the relationship may be nonlinear outside the range spanned in Table 9.5 (Knutti et al., 2005).

Based on the methods outlined above and explained in Section 9.7.2 below, Table 9.5 shows effective ERF, ECS, TCR and feedback strengths for the CMIP5 ensemble. The two estimates of ERF agree with each other to within 5% for six models (CanESM2, INM-CM4, IPSL-CM5A-LR, MIROC5, MPI-ESM-LR and MPI-ESM-P), although the deviation exceeds 10% for four models (CCSM4, CSIRO-Mk3-6-0, HadGEM2-ES, and MRI-CGCM3) and is indicative of deviations from the basic assumptions underlying one or both ERF estimation methods. However, the mean difference of 0.3 W m^{-2} between the two methods for diagnosing ERF is only about half of the ensemble standard deviation of 0.5 W m^{-2}, or 15% of the mean value for ERF by CO_2 using fixed SSTs. ECS and TCR vary across the ensemble by a factor of approximately 2. The multi-model ensemble mean in ECS is 3.2°C, a value nearly identical to that for CMIP3, while the CMIP5 ensemble range is 2.1°C to 4.7°C, a spread which is also nearly indistinguishable from that for CMIP3. While every CMIP5 model whose heritage can

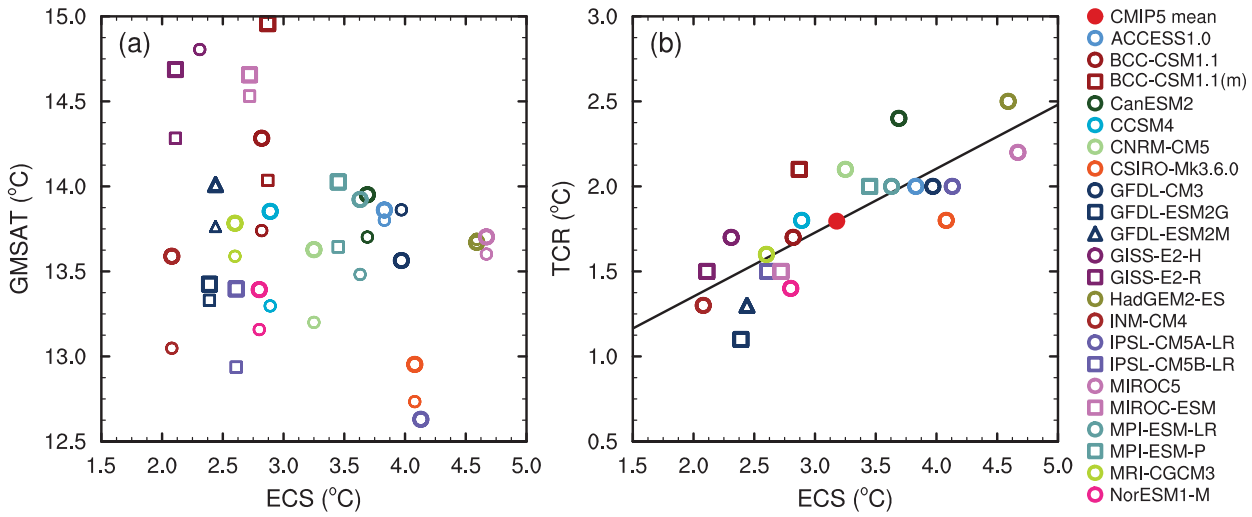

Figure 9.42 | (a) Equilibrium climate sensitivity (ECS) against the global mean surface temperature of CMIP5 models, both for the period 1961–1990 (larger symbols, cf. Figure 9.8, Table 9.5) and for the pre-industrial control runs (smaller symbols). (b) Equilibrium climate sensitivity against transient climate response (TCR). The ECS and TCR information are based on Andrews et al. (2012) and Forster et al. (2013) and updated from the CMIP5 archive.

Table 9.5 | Effective radiative forcing (ERF), climate sensitivity and climate feedbacks estimated for the CMIP5 AOGCMs (see Table 9.1 for model details). ERF, equilibrium climate sensitivity (ECS) and transient climate response (TCR) are based on Andrews et al. (2012) and Forster et al. (2013) and updated from the CMIP5 archive. The ERF entries are calculated according to Hansen et al. (2005) using fixed sea surface temperatures (SSTs) and Gregory et al. (2004) using regression. ECS is calculated using regressions following Gregory et al. (2004). TCR is calculated from the CMIP5 simulations with 1% CO_2 increase per year (Taylor et al., 2012b), using the 20-year mean centred on the year of CO_2 doubling. The climate sensitivity parameter and its inverse, the climate feedback parameter, are calculated from the regression-based ERF and the ECS. Strengths of the individual feedbacks are taken from Vial et al. (2013), following Soden et al. (2008) and using radiative kernel methods with two different kernels. The sign convention is such that a positive entry for an individual feedback marks a positive feedback; the sum of individual feedback strengths must hence be multiplied by –1 to make it comparable to the climate feedback parameter. The entries for radiative forcing and equilibrium climate sensitivity were obtained by dividing by two the original results, which were obtained for CO_2 quadrupling. ERF and ECS for BNU-ESM are from Vial et al. (2013).

Model	Effective Radiative Forcing 2 × CO_2 (W m^{-2})		Equilibrium Climate Sensitivity (°C)	Transient Climate Response (°C)	Climate Sensitivity Parameter (°C (W m^{-2}) $^{-1}$)	Climate Feedback Parameter (W m^{-2} °C^{-1})	Planck Feedback (W m^{-2} °C^{-1})	Water Vapour Feedback (W m^{-2} °C^{-1})	Lapse Rate Feedback (W m^{-2} °C^{-1})	Surface Albedo Feedback (W m^{-2} °C^{-1})	Cloud Feedback (W m^{-2} °C^{-1})
	Fixed SST	Regression									
ACCESS1.0	n.a.	3.0	3.8	2.0	1.3	0.8	n.a.	n.a.	n.a.	n.a.	n.a.
ACCESS1.3	n.a.	n.a.	n.a.	1.7	n.a.	n.a.	n.a.	n.a.	n.a.	n.a.	n.a.
BCC–CSM1.1	n.a.	3.2	2.8	1.7	0.9	1.1	n.a.	n.a.	n.a.	n.a.	n.a.
BCC–CSM1.1(m)	n.a.	3.6	2.9	2.1	0.8	1.2	n.a.	n.a.	n.a.	n.a.	n.a.
BNU–ESM	n.a.	3.9	4.1	2.6	1.1	1.0	–3.1	1.4	–0.2	0.4	0.1
CanESM2	3.7	3.8	3.7	2.4	1.0	1.0	–3.2	1.7	–0.6	0.3	0.5
CCSM4	4.4	3.6	2.9	1.8	0.8	1.2	–3.2	1.5	–0.4	0.4	–0.4
CESM1(BGC)	n.a.	n.a.	n.a.	1.7	n.a.	n.a.	n.a.	n.a.	n.a.	n.a.	n.a.
CESM1(CAM5)	n.a.	n.a.	n.a.	2.3	n.a.	n.a.	n.a.	n.a.	n.a.	n.a.	n.a.
CNRM–CM5	n.a.	3.7	3.3	2.1	0.9	1.1	n.a.	n.a.	n.a.	n.a.	n.a.
CSIRO–Mk3.6.0	3.1	2.6	4.1	1.8	1.6	0.6	n.a.	n.a.	n.a.	n.a.	n.a.
FGOALS–g2	n.a.	n.a.	n.a.	1.4	n.a.	n.a.	n.a.	n.a.	n.a.	n.a.	n.a.
GFDL–CM3	n.a.	3.0	4.0	2.0	1.3	0.8	n.a.	n.a.	n.a.	n.a.	n.a.
GFDL–ESM2G	n.a.	3.1	2.4	1.1	0.8	1.3	n.a.	n.a.	n.a.	n.a.	n.a.
GFDL–ESM2M	n.a.	3.4	2.4	1.3	0.7	1.4	n.a.	n.a.	n.a.	n.a.	n.a.
GISS–E2–H	n.a.	3.8	2.3	1.7	0.6	1.7	n.a.	n.a.	n.a.	n.a.	n.a.
GISS–E2–R	n.a.	3.8	2.1	1.5	0.6	1.8	n.a.	n.a.	n.a.	n.a.	n.a.
HadGEM2–ES	3.5	2.9	4.6	2.5	1.6	0.6	–3.2	1.4	–0.5	0.3	0.4
INM–CM4	3.1	3.0	2.1	1.3	0.7	1.4	–3.2	1.7	–0.7	0.3	0
IPSL–CM5A–LR	3.2	3.1	4.1	2.0	1.3	0.8	–3.3	1.9	–1	0.2	1.2
IPSL–CM5A–MR	n.a.	n.a.	n.a.	2.0	n.a.	n.a.	n.a.	n.a.	n.a.	n.a.	n.a.
IPSL–CM5B–LR	n.a.	2.7	2.6	1.5	1.0	1.0	n.a.	n.a.	n.a.	n.a.	n.a.
MIROC5	4.0	4.1	2.7	1.5	0.7	1.5	–3.2	1.7	–0.6	0.3	0.1
MIROC–ESM	n.a.	4.3	4.7	2.2	1.1	0.9	n.a.	n.a.	n.a.	n.a.	n.a.
MPI–ESM–LR	4.3	4.1	3.6	2.0	0.9	1.1	–3.3	1.8	–0.9	0.3	0.5
MPI–ESM–MR	n.a.	n.a.	n.a.	2.0	n.a.	n.a.	n.a.	n.a.	n.a.	n.a.	n.a.
MPI–ESM–P	4.3	4.3	3.5	2.0	0.8	1.2	n.a.	n.a.	n.a.	n.a.	n.a.
MRI–CGCM3	3.6	3.2	2.6	1.6	0.8	1.2	–3.2	1.6	–0.6	0.3	0.2
NorESM1–M	n.a.	3.1	2.8	1.4	0.9	1.1	–3.2	1.6	–0.5	0.3	0.2
NorESM1–ME	n.a.	n.a.	n.a.	1.6	n.a.	n.a.	n.a.	n.a.	n.a.	n.a.	n.a.
Model mean	**3.7**	**3.4**	**3.2**	**1.8**	**1.0**	**1.1**	**–3.2**	**1.6**	**–0.6**	**0.3**	**0.3**
90% uncertainty	**±0.8**	**±0.8**	**±1.3**	**±0.6**	**±0.5**	**±0.5**	**±0.1**	**±0.3**	**±0.4**	**±0.1**	**±0.7**

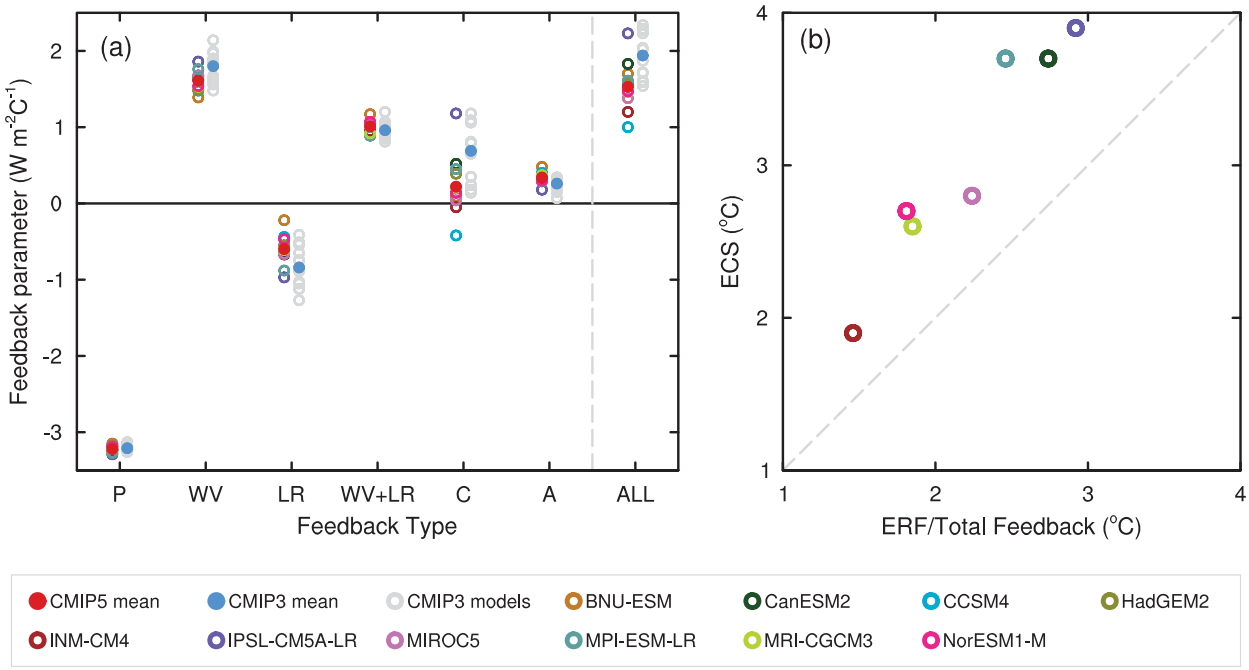

Figure 9.43 | (a) Strengths of individual feedbacks for CMIP3 and CMIP5 models (left and right columns of symbols) for Planck (P), water vapour (WV), clouds (C), albedo (A), lapse rate (LR), combination of water vapour and lapse rate (WV+LR) and sum of all feedbacks except Planck (ALL), from Soden and Held (2006) and Vial et al. (2013), following Soden et al. (2008). CMIP5 feedbacks are derived from CMIP5 simulations for abrupt fourfold increases in CO_2 concentrations ($4 \times CO_2$). (b) ECS obtained using regression techniques by Andrews et al. (2012) against ECS estimated from the ratio of CO_2 ERF to the sum of all feedbacks. The CO_2 ERF is one-half the $4 \times CO_2$ forcings from Andrews et al. (2012), and the total feedback (ALL + Planck) is from Vial et al. (2013).

be traced to CMIP3 shows some change in ECS, there is no discernible systematic tendency. This broad similarity between CMIP3 and CMIP5 and the good agreement between different methods where they were applied to the same atmospheric GCM indicate that the uncertainty in methodology is minor compared to the overall spread in ECS. The change in TCR from CMIP3 to CMIP5 is generally of the same sign but of smaller magnitude compared to the change in ECS. The relationship between ECS and an estimates derived from total feedbacks are discussed in Section 9.7.2.

Although ECS can vary with global mean surface temperature owing to the temperature dependencies of the various feedbacks (Colman and McAvaney, 2009; cf. Section 9.7.2), Figure 9.42 shows no discernible correlation for the CMIP5 historical temperature ranges, a fact that suggests that ECS is less sensitive to errors in the current climate than to other sources of uncertainty.

9.7.2 Understanding the Range in Model Climate Sensitivity: Climate Feedbacks

The strengths of individual feedbacks for the CMIP3 and CMIP5 models are compared in Figure 9.43. The feedbacks are generally similar between CMIP3 and CMIP5, and the water vapour, lapse rate, and cloud feedbacks are assessed in detail in Chapter 7. The surface albedo feedback is assessed here to be *likely* positive. There is *high confidence* that the sum of all feedbacks (excluding the Planck feedback) is positive. Advances in estimating and understanding each of the feedback parameters in Table 9.5 are described in detail below (see also Chapters 7 and 8).

9.7.2.1 Role of Humidity and Lapse Rate Feedbacks in Climate Sensitivity

The compensation between the water vapour and lapse-rate feedbacks noted in the CMIP3 models is still present in the CMIP5 models, and possible explanations of the compensation have been developed (Ingram, 2010; Ingram, 2013). New formulations of the feedbacks, replacing specific with relative humidity, eliminate most of the cancellation between the water vapour and lapse rate feedbacks and reduce the inter-model scatter in the individual feedback terms (Held and Shell, 2012).

9.7.2.2 Role of Surface Albedo in Climate Sensitivity

Analysis of observed declines in sea ice and snow coverage from 1979 to 2008 suggests that the NH albedo feedback is between 0.3 and 1.1 W m^{-2} °C^{-1} (Flanner et al., 2011). This range is substantially above the global feedback of 0.3 ± 0.1 W m^{-2} °C^{-1} of the CMIP5 models analysed in Table 9.5. One possible explanation is that the CMIP5 models underestimate the strength of the feedback as did the CMIP3 models based upon the systematic errors in simulated sea ice coverage decline relative to observed rates (Boe et al., 2009b).

9.7.2.3 Role of Cloud Feedbacks in Climate Sensitivity

Cloud feedbacks represent the main cause for the range in modelled climate sensitivity (Chapter 7). The spread due to inter-model differences in cloud feedbacks is approximately 3 times larger than the spread contributed by feedbacks due to variations in water vapour and lapse

rate combined (Dufresne and Bony, 2008), and is a primary factor governing the range of climate sensitivity across the CMIP3 ensemble (Volodin, 2008a). Differences in equilibrium and effective climate sensitivity are due primarily to differences in the shortwave cloud feedback (Yokohata et al., 2008).

In perturbed ensembles of three different models, the primary cloud-related factor contributing to the spread in equilibrium climate sensitivity is the low-level shortwave cloud feedback (Yokohata et al., 2010; Klocke et al., 2011). Changes in the high-altitude clouds also induce climate feedbacks due to the large areal extent and significant longwave cloud radiative effects of tropical convective cloud systems. In experiments with perturbed physics ensembles of AOGCMs, the parameterization of ice fall speed also emerges as one of the most important determinants of climate sensitivity (Sanderson et al., 2008a, 2010; Sexton et al., 2012). Other non-microphysical feedback mechanisms are detailed in Chapter 7.

Cloud feedbacks in AOGCMs are generally positive or near neutral (Shell et al., 2008; Soden et al., 2008), as evidenced by the net positive or neutral cloud feedbacks in all of the models examined in a multi-thousand member ensemble of AOGCMs constructed by parameter perturbations (Sanderson et al., 2010). The sign of cloud feedbacks in the current climate deduced from observed relationships between SSTs and TOA radiative fluxes are discussed further in Section 7.2.5.7.

9.7.2.4 Relationship of Feedbacks to Modelled Climate Sensitivity

The ECS can be estimated from the ratio of forcing to the total climate feedback parameter. This approach is applicable to simulations in which the net radiative balance is much smaller than the forcing and hence the modelled climate system is essentially in equilibrium. This approach can also serve to check the internal consistency of estimates of the ECS, forcing, and feedback parameters obtained using independent methods. The relationship between ECS from Andrews et al. (2012) and estimates of ECS obtained from the ratio of forcings to feedbacks is shown in Figure 9.43b. The forcings are estimated using both regression and fixed SST techniques (Gregory et al., 2004; Hansen et al., 2005) by Andrews et al. (2012) and the feedbacks are calculated using radiative kernels (Soden et al., 2008). On average, the ECS from forcing to feedback ratios underestimate the ECS from Andrews et al. (2012) by 25% and 35%, or up to 50% for individual models, using fixed-SST and regression forcings, respectively.

9.7.2.5 Relationship of Feedbacks to Uncertainty in Modelled Climate Sensitivity

Objective methods for perturbing uncertain model parameters to optimize performance relative to a set of observational metrics have shown a tendency toward an increase in the mean and a narrowing of the spread of estimated climate sensitivity (Jackson et al., 2008a). This tendency is opposed by the effects of structural biases related to incomplete process representations in GCMs. If common structural biases are replicated across models in a MME (cf. Section 9.2.2.7), the most likely sensitivity for the MME tends to shift towards lower sensitivities while the possibility of larger sensitivities increases at the same time (Lemoine, 2010). Following Schlesinger and Mitchell (1987), Roe and Baker (2007) suggest that symmetrically distributed uncertainties in feedbacks lead to inherently asymmetrical uncertainties in climate sensitivity with increased probability in extreme positive values of the sensitivity. Roe and Baker (2007) conclude that this relationship makes it extremely difficult to reduce uncertainties in climate sensitivity through incremental improvements in the specification of feedback parameters. While subsequent analysis has suggested that this finding could be an artifact of the statistical formulation (Hannart et al., 2009) and linearization (Zaliapin and Ghil, 2010) of the relationship between feedback and sensitivity adopted by (Roe and Baker, 2007), these issues remain unsettled (Roe and Armour, 2011; Roe and Baker, 2011).

9.7.3 Climate Sensitivity and Model Performance

Despite the range in equilibrium sensitivity of 2.1°C to 4.4°C for CMIP3 models, they reproduce the global surface air temperature anomaly of 0.76°C over 1850–2005 to within 25% relative error. The relatively small range of historical climate response suggests that there is another mechanism, for example a compensating non-GHG forcing, present in the historical simulations that counteracts the relatively large range in sensitivity obtained from idealized experiments forced only by increasing CO_2. One possible mechanism is a systematic negative correlation across the multi-model ensemble between ECS and anthropogenic aerosol forcing (Kiehl, 2007; Knutti, 2008; Anderson et al., 2010). A second possible mechanism is a systematic overestimate of the mixing between the oceanic mixed layer and the full depth ocean underneath (Hansen et al., 2011). However, despite the same range of ECS in the CMIP5 models as in the CMIP3 models, there is no significant relationship across the CMIP5 ensemble between ECS and the 20th-century ERF applied to each individual model (Forster et al., 2013). This indicates a lesser role of compensating ERF trends from GHGs and aerosols in CMIP5 historical simulations than in CMIP3. Differences in ocean heat uptake also do not appreciably affect the spread in projected changes in global mean temperature by 2095 (Forster et al., 2013).

9.7.3.1 Constraints on Climate Sensitivity from Earth System Models of Intermediate Complexity

An EMIC intercomparison (Eby et al., 2013; Zickfeld et al., 2013) allows an assessment of model response characteristics, including ECS, TCR, and heat uptake efficiency (Table 9.6). In addition, Bayesian methods applied to PPE experiments using EMICs have estimated uncertainty in model response characteristics (see Box 12.2) based on simulated climate change in 20th century, past millennia, and LGM scenarios. Here, the range of response metrics (Table 9.6) described for default model configurations (Eby et al., 2013) indicates consistency with the CMIP5 ensemble.

9.7.3.2 Climate Sensitivity During the Last Glacial Maximum

Climate sensitivity can also be explored in another climatic context. The AR4 assessed attempts to relate simulated LGM changes in tropical SST to global climate sensitivity (Hegerl et al., 2007; Knutti and Hegerl, 2008). LGM temperature changes in the tropics (Hargreaves et al., 2007), but not in Antarctica (Hargreaves et al., 2012), have been

Table 9.6 | Model response metrics for EMICs in Table 9.2. TCR_{2X}, TCR_{4X} and ECS_{4X} are the changes in global average model surface air temperature from the decades centred at years 70, 140 and 995 respectively, from the idealized 1% increase to 4 × CO_2 experiment. The ocean heat uptake efficiency, κ_{4X}, is calculated from the global average heat flux divided by TCR_{4X} for the decade centred at year 140, from the same idealized experiment. ECS_{2x} was calculated from the decade centred about year 995 from a 2 × CO_2 pulse experiment. (Data from Eby et al., 2013.)

Model	TCR_{2X} (°C)	ECS_{2x}(°C)	TCR_{4X} (°C)	ECS_{4X} (°C)	κ_{4X} (W m^{-2} $°C^{-1}$)
Bern3D	2.0	3.3	4.6	6.8	0.58
CLIMBER2	2.1	3.0	4.7	5.8	0.84
CLIMBER3	1.9	3.2	4.5	5.9	0.93
DCESS	2.1	2.8	3.9	4.8	0.72
FAMOUS	2.3	3.5	5.2	8.0	0.55
GENIE	2.5	4.0	5.4	7.0	0.51
IAP RAS CM	1.6	—	3.7	4.3	—
IGSM2	1.5	1.9	3.7	4.5	—
LOVECLIM1.2	1.2	2.0	2.1	3.5	1.17
MESMO	2.4	3.7	5.3	6.9	0.55
MIROC-lite	1.6	2.4	3.6	4.6	0.66
MIROC-lite-LCM	1.6	2.8	3.7	5.5	1.00
SPEEDO	0.8	3.6	2.9	5.2	0.84
UMD	1.6	2.2	3.2	4.3	—
Uvic	1.9	3.5	4.3	6.6	0.92
EMIC mean	1.8	3.0	4.0	5.6	0.8
EMIC range	0.8–2.5	1.9–4.0	2.1–5.4	3.5–8.0	0.5–1.2

shown to scale well with climate sensitivity because the signal is mostly dominated by CO_2 forcing in these regions (Braconnot et al., 2007b; Jansen et al., 2007). The analogy between the LGM climate sensitivity and future climate sensitivity is, however, not perfect (Crucifix, 2006). In a single-model ensemble of simulations, the magnitudes of the LGM cooling and the warming induced by a doubling of CO_2 are nonlinear in the forcings applied (Hargreaves et al., 2007). Differences in the cloud radiative feedback are at the origin of this asymmetric response to equivalent positive and negative forcings (Yoshimori et al., 2009). There is thus still *low confidence* that the regional LGM model-data comparisons can be used to evaluate model climate sensitivity. However, even if the results do not scale perfectly with equilibrium or transient climate sensitivity, the LGM simulations allow the identification of the different feedback factors that contributed to the LGM global cooling (Yoshimori et al., 2011) and model spread in these feedbacks. The largest spread in LGM model feedbacks is found for the shortwave cloud feedback, just as for the modern climate. This correspondence between LGM and modern climates adds to the *high confidence* that the shortwave cloud feedback is the dominant source of model spread in climate sensitivity (cf. Section 5.3.3).

9.7.3.3 Constraints on Equilibrium Climate Sensitivity from Climate-Model Ensembles and Observations

The large scale climatological information available has so far been insufficient to constrain model behaviour to a range tighter than CMIP3, at least on a global scale. Sanderson and Knutti (2012) suggest that much of the available and commonly used large scale observations have already been used to develop and evaluate models and are therefore of limited value to further constrain climate sensitivity or TCR. The assessed literature suggests that the range of climate sensitivities and transient responses covered by CMIP3/5 cannot be narrowed significantly by constraining the models with observations of the mean climate and variability, consistent with the difficulty of constraining the cloud feedbacks from observations (see Chapter 7). Studies based on PPE and CMIP3 support the conclusion that a credible representation of the mean climate and variability is very difficult to achieve with equilibrium climate sensitivities below 2°C (Piani et al., 2005; Stainforth et al., 2005; Sanderson et al., 2008a, 2008b; Huber et al., 2011; Klocke et al., 2011; Fasullo and Trenberth, 2012). High climate sensitivity values above 5°C (in some cases above 10°C) are found in the PPE based on HadAM/HadCM3. Several recent studies find that such high values cannot be excluded based on climatological constraints, but comparison with observations shows the smallest errors for many fields if ECS is between 3 and 4°C (Piani et al., 2005; Knutti et al., 2006; Rodwell and Palmer, 2007; Sanderson et al., 2008a, 2008b, 2010; Sanderson, 2011, 2013).

9.8 Relating Model Performance to Credibility of Model Applications

9.8.1 Synthesis Assessment of Model Performance

This chapter has assessed the performance of individual climate models as well as the multi-model mean. In addition, changes between models available now and those that were available at the time of the AR4 have been documented. The models display a range of abilities to